RSC Advances

ROYAL SOCIETY OF CHEMISTRY

www.rsc.org/advances

RSC Advances

RSCPublishing

PAPER

Investigation of Hydrogen Bonding Patterns in A Series of Multi-component Molecular Solids Formed by Tetrabromoterephthalic Acid with Selected N-heterocycles

Cite this: DOI: 10.1039/xoxxoooooox

Received ooth January 2012,
Accepted ooth January 2012

DOI: 10.1039/xoxxoooooox

www.rsc.org/

Lei Wang,* Wenyan Xu, Yanjing Hu, Yanyan Pang, Faqiang Liu, Yu Yang*

The supramolecular reactions of tetrabromoterephthalic acid (H_2-TBTA) with a series of N-heterocycles afford eight new complexes, namely, [(H_2-BTAH)$_2$·(TBTA)·(H_2-TBTA)] **(1)**, [(H_2-Bim)$_2$·(TBTA)·(H_2-TBTA)·2H_2O] **(2)**, [(H-8-HQ)$_2$·(TBTA)·3H_2O] **(3)**, [(5-NO_2-phen)$_2$·(H_2-TBTA)] **(4)**, [(4,6-DHP)$_2$·(H_2-TBTA)·2H_2O] **(5)**, [(H_2-2,4-DMI)$_2$·(TBTA)·(H_2-TBTA)$_2$] **(6)**, [(H_2-3,5-DMP)$_2$·(TBTA)] **(7)**, and [(H-4-CNpy)$_2$·(TBTA)·(H_2-TBTA)] **(8)** (H-BTAH = 1H-Benzotriazole, H-Bim = 1H-Benzimidazole, 8-HQ = 8-Hydroxyquinoline, 5-NO_2-phen = 5-Nitro-1,10-phenanthroline, 4,6-DHP = 4,6-Dihydroxypyrimidine, H-2,4-DMI = 2,4-Dimethylimidazole, H-3,5-DMP = 3,5-Dimethylpyrazole, and 4-CNpy = 4-Cyanopyridine), which have been prepared under mild and identical reaction conditions in a mixture of distilled water and ethanol. All the complexes were fully characterized by single crystal X-ray diffraction analysis, elemental analysis, infrared spectroscopy (IR), and thermogravimetric analysis (TGA). Combining the various N-containing ligands and the diversity of the hydrogen bonds, the eight crystals display amusing structural characteristics. Of this, complex **3** forms three-dimensional (3D) network through the C–H···Br, whilst the O–H···Br consist in the 3D construction of compound **2**. Complexes **4-8** generate a 3D supramolecular structure by large amounts of hydrogen bonds. In crystal **1**, the π–π stacking interactions play an important part in the 3D network. The thermal stability of crystals **1**-**8** has been investigated by thermogravimetric analysis (TGA) of mass loss.

Introduction

The rational design and synthesis of organic solids from molecular components is one of the main focuses in the field of crystal engineering,[1] not only because of their intriguing structures but also because of their potential applications in drug delivery,[2] sensing,[3] and nonlinear optics.[4] Self-assembly is the fundamental feature of natural and biological processes with noncovalent interactions acting as tools to accomplish these tasks,[5] which normally contain hydrogen bonds, electrostatic interactions, van der Waals forces, π–π stacking interactions, halogen bonds[6] and so on. Currently, the strong hydrogen bonds O–H···O and N–H···O are very prevalent in controlling molecular assembly during crystallization.[7] Furthermore, the weak C–H···O and C–H···N hydrogen bonds also play an important part in distorting and modifying the structure predicted.[8] In the past two decades, the halogen bonds especially the C–H···halogen hydrogen bonds and halogen···halogen interactions gain widely attention[9] despite the first unequivocal report on the halogen bonding can be traced back to 1863 when Guthrie described the formation of the complex NH_3···I_2.[10]

Nowadays, more and more researchers are focus on the halogen-substituted compounds,[11] because chemists recognized that the halogen bonds play a significant role in crystal packing in many halogen-containing organic compounds[12] due to its highly directional, as well as fully hydrophobic characteristics.[13] Four halogen-substituted dicarboxylic acid as a good ligand has a lot of advantages, which is applied to metal-organic frameworks (MOFs) and supramolecular chemistry.[14] However, up to now, the systematic studies concerned with four halogen-substituted dicarboxylic acid are still relatively scarce. The results of our previous studies[14k,14l] show that tetrabromoterephthalic acid exhibits the special ability to form the organic solids through the noncovalent interactions particularly the halogen bond C–H···F.

In order to continue our previous work and explore the role of the halogen bonds in the synthesis of the supramolecular, we select

Key Laboratory of Eco-chemical Engineering, Ministry of Education, Laboratory of Inorganic Synthesis and Applied Chemistry, College of Chemistry and Molecular Engineering, Qingdao University of Science and Technology, Qingdao 266042, P. R. China. E-mail: inorchemwl@126.com; yangyu9039@163.com; Fax: (+86) 532-840-22681

† Electronic Supplementary Information (ESI) available: IR, TGA, DSC data and synthons XIV–XXXI about this work. CCDC reference numbers 1016043-1016050. For ESI and crystallographic data in CIF or other electronic format see DOI: XXXXXXX

tetrabromoterephthalic acid (H_2-TBTA) as dicarboxylic acid ligand, 1H-Benzotriazole, 1H-Benzimidazole, 8-Hydroxyquinoline, 5-Nitro-1,10-phenanthroline, 4,6-Dihydroxypyrimidine, 2,4-Dimethylimidazole, 3,5-Dimethylpyrazole, 4-Cyanopyridine are employed as N-heterocycles (**Scheme 1**). In this article, eight new complexes have been obtained through the noncovalent interactions. Meanwhile, we discovered the structural characterization, and the thermal stabilities of these complexes have been also investigated in the solid state.

Experimental Section

Materials All the reagents and solvents were purchased commercially available and used as received without further purification. 1H-Benzotriazole, 1H-Benzimidazole, 8-Hydroxyquinoline, 5-Nitro-1,10-phenanthroline, 4,6-Dihydroxypyrimidine, 2,4-Dimethylimidazole, 3,5-Dimethylpyrazole, 4-Cyanopyridine and tetrabromoterephthalic acid, were obtained from Energy Chemical.

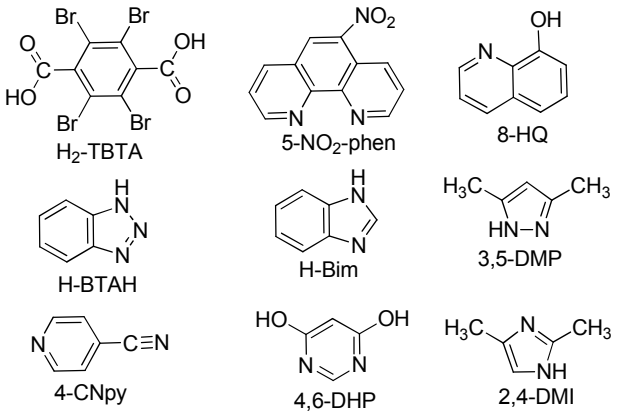

Scheme 1. Molecular Structures in This Work.

Physical Measurements Melting point measurements were carried out using a WRS-1B digital thermal apparatus without correction and refer to the temperature at the start of the melt. The FT–IR spectra were recorded on a Nicolet Impact 410 FTIR in the range of 4000–400 cm^{-1} using the KBr disc technique. Absorptions are denoted as follows: strong (s), medium (m), and weak (w) in the synthesis section. Carbon, hydrogen, and nitrogen contents were performed with a Perkin–Elmer 2400 elemental analyzer. Thermogravimetric analysis (TGA) was performed from room temperature to 900℃ by using a Perkin-Elmer TGA–7 TG analyzer with a heating rate of 10℃/min in a N_2 atmosphere. The eight novel crystals were composed as follows.

Synthesis of the complexes 1–8

Synthesis of $[(C_6H_6N_3^+)_2\cdot(C_8Br_4O_4^{2-})\cdot(C_8H_2Br_4O_4)]$ Salt, (1) A solution of H_2-TBTA (42.8 mg, 0.10 mmol) was prepared in 5 mL of ethanol. 5mL distilled water solution of 1H-Benzotriazole (23.8 mg, 0.20 mmol) was added to the above solution. The resulting solution was stirred for 15 min and kept at room temperature for crystallization. Colorless, block crystals were gained after two weeks. The obtained crystals were separated from the mother solution by filtration, washed with ethanol-distilled water solution (v/v = 1:1), and dried under vacuum. Crystals were obtained in 58.7% yield by filtration and were found to be suitable for single–crystal X-ray diffraction analysis. m.p.: 204℃. Anal. Calcd (%) for $C_{21}H_{21}Br_4N_2O_7$ **(1)**: C 34.38, H 2.86, N 3.82; found : C 34.16, H 3.04, N 3.66. IR (KBr pellet, cm^{-1}) : 3436(m), 3111(w), 2963(w), 2918(w), 2852(w), 2520(w), 1616(m), 1405(m), 1328(m), 1304(m), 1237(m), 1221(m), 1180(m), 1136(m), 1085(m), 1008(w), 996(w), 937(w), 876(m), 805(m), 749(s), 742(s), 661(m), 621(s), 563(s), 536(s), 520(s), 425(m).

Synthesis of $[(C_7H_7N_2^+)_2\cdot(C_8Br_4O_4^{2-})\cdot(C_8H_2Br_4O_4)\cdot 2H_2O]$ Hydrate (2) Benzimidazole (11.8 mg, 0.10 mmol) was dissolved in 5 mL of ethanol followed by the addition of 5 mL distilled water solution of H_2-TBTA (42.8 mg, 0.10 mmol). The resulting colorless solution was stirred for 15 min and kept at room temperature for crystallization. Colorless block shaped crystals after three weeks in about 67.3% yield were filtered and washed with ethanol-distilled water solution (v/v = 1:1), then dried in vacuum desiccators. Crystals were found to be suitable for single-crystal X-ray diffraction analysis. m.p.: 246℃. Anal. Calcd (%) for $C_{30}H_{20}Br_8N_4O_{10}$ **(2)**: C 29.13, H 1.62, N 4.53; found : C 28.95, H 1.68, N 4.48. IR (KBr pellet, cm^{-1}) : 3586(m), 3385(m), 3154(w), 3075(w), 2970(w), 2829(m), 2755(m), 2684(m), 2593(m), 1711(m), 1635(s), 1626(s), 1611(s), 1449(m), 1422(m), 1378(m), 1330(s), 1303(s), 1241(s), 1191(m), 1153(w), 1081(m), 1007(w), 985(w), 923(w), 876(w), 848(m), 836(m), 785(w), 746(s), 691(w), 619(s), 608(m), 576(m), 557(m), 523(m), 420(m).

Synthesis of $[(C_9H_8NO^+)_2\cdot(C_8Br_4O_4^{2-})\cdot 3H_2O]$ Hydrate, (3) 5 mL distilled water solution of 8-Hydroxyquinoline (29.0 mg, 0.20 mmol) was mixed to 5 mL ethanol solution of H_2-TBTA (42.8 mg, 0.10 mmol), and the yellow solution was stirred for 15 min then kept the turbid liquid overnight at room temperature. In the next day, filter the turbid liquid and retain the clear homogeneous solution at room temperature for slow evaporation. Primrose yellow block shaped crystals in about 68%yield were obtained after three weeks and separated from the mother liquor. Washed the crystals with the acetonitrile-distilled water solution (v/v = 1:1) and dried under vacuum. Crystals were obtained to be suitable for single-crystal X-ray diffraction analysis. m.p.: 266 ℃ . Anal. Calcd (%) for $C_{26}H_{22}Br_4N_2O_9$ **(3)**: C 37.77, H 2.66, N 3.39; found : C 37.14, H 2.88, N 3.12. IR (KBr pellet, cm^{-1}) : 3450(m), 3236(m), 3070(m), 3056(m), 3023(m), 2918(m), 2792(m), 2690(m), 2583(m), 1636(m), 1600(s), 1585(s), 1564(s), 1504(m), 1475(m), 1423(s), 1400(s), 1323(s), 1301(s), 1264(m), 1212(m), 1177(m), 1143(m), 1099(m), 1083(m), 1035(w), 987(m), 938(w), 890(w), 824(s), 802(m), 773(m), 713(m), 701(m), 623(m), 564(s), 542(m), 520(m), 489(m), 475(m), 416(m).

Synthesis of $[(C_{12}H_7N_3O_2)_2\cdot(C_8H_2Br_4O_4)]$ Cocrystal, (4) H_2-TBTA (42.8 mg, 0.10 mmol) and 5-Nitro-1,10-phenanthroline (11.3 mg, 0.05 mmol) were taken in a 2:1 molar ratio and dissolved in ethanol-distilled water solution (v/v = 1:1, 10 mL), the solution was stirred for 15 min and obtained turbid liquid overnight at room temperature. In the next day, filter the turbid liquid and retain the clear homogeneous solution at room temperature for slow evaporation. Good quality orange crystals, suitable for diffraction, were gained after one week as the solution slow evaporation at room temperature.

The obtained crystals were picked up from the mother liquor by filtration, use the ethanol-distilled water solution (v/v = 1:1) to wash, and dried in vacuum desiccators. Crystals were obtained in 56.7% yield by filtration and were found to be suitable for single–crystal X-ray diffraction analysis. m.p.: 236 ℃ . Anal. Calcd (%) for $C_{32}H_{16}Br_4N_6O_8$ **(4)**: C 41.20, H 1.72, N 9.01; found : C 40.79, H 1.89, N 8.87. IR (KBr pellet, cm^{-1}) : 3436(m), 3217(w), 3096(w), 2872(w), 2570(w), 2477(w), 1713(s), 1637(s), 1617(s), 1593(m), 1541(s), 1531(s), 1497(m), 1467(m), 1450(w), 1435(w), 1417(w), 1346(m), 1332(s), 1306(s), 1231(s), 1177(s), 1086(s), 979(m), 920(m), 875(m), 830(m), 817(m), 794(s), 777(s), 723(m), 701(m), 620(m), 557(s), 525(m), 486(m), 413(m).

Synthesis of $[(C_4H_4N_2O_2)_2\cdot(C_8H_2Br_4O_4)\cdot 2H_2O]$ Cocrystal, (5) 4,6-Dihydroxypyrimidine (5.6 mg, 0.05 mmol) was dissolved in 5 mL of distilled water, and H_2-TBTA (42.8 mg, 0.10 mmol) was dissolved in 5 mL of ethanol. Both the solutions were mixed and stirred at room temperature. About 15 min later obtained turbid liquid overnight at room temperature. In the next day, filter the turbid liquid and retain the clear homogeneous solution at room temperature for slow evaporation. Two weeks later crystals started coming out and the yield about 73%. It was further filter and washed with ethanol-distilled water (v/v = 1:1), and dried in vacuum desiccators. Crystals were found to be suitable for single–crystal X-ray diffraction analysis. m.p.: 214 ℃ . Anal. Calcd (%) for $C_{16}H_{14}Br_4N_4O_{10}$ **(5)**: C 25.88, H 1.89, N 7.55; found : C 25.76, H 2.04, N 7.36. IR (KBr pellet, cm^{-1}) : 3532(m), 3381(m), 3078(m), 2727(m), 2611(m), 1997(w), 1683(s), 1660(s), 1592(s), 1568(m), 1457(w), 1376(m), 1358(m), 1334(m), 1307(s), 1264(m), 1207(m), 1138(m), 1088(m), 992(w), 925(m), 818(m), 788(m), 733(w), 695(m), 600(m), 574(m), 527(s), 459(s), 445(m).

Synthesis of $[(C_5H_9N_2^+)_2\cdot(C_8Br_4O_4^{2-})\cdot(C_8H_2Br_4O_4)_2]$ Salt, (6) 9.6 mg of 2,4-Dimethylimidazole (0.10 mmol) was dissolved in 5mL of distilled water and 5 mL ethanol of H_2-TBTA (42.8 mg, 0.10 mmol) was added to this solution and stirred for 15 min to get a homogeneous solution. The resultant solution was allowed to evaporate slowly at room temperature, colorless block-like crystals suitable for X-ray diffraction were obtained in about 62% yield within two weeks. The crystals were separated from the mother liquor by filtration, washed with ethanol-distilled water solution (v/v = 1:1), and dried under vacuum. Crystals were obtained in 46.8% yield by filtration and were found to be suitable for single-crystal X-ray diffraction analysis. m.p.: 222 ℃ . Anal. Calcd (%) for $C_{34}H_{22}Br_{12}N_4O_{12}$ **(6)**: C 24.92, H 1.34, N 3.42; found : C 24.76, H 1.50, N 3.28. IR (KBr pellet, cm^{-1}) : 3436(m), 3150(m), 3097(m), 2975(m), 2931(m), 2755(m), 2667(w), 2593(w), 1749(s), 1690(m), 1649(m), 1559(m), 1437(m), 1391(s), 1333(s), 1306(s), 1241(s), 1089(m), 1079(m), 1008(m), 968(m), 885(m), 798(m), 787(m), 719(m), 692(m), 628(m), 589(m), 553(m), 520(m).

Synthesis of $[(C_5H_9N_2^+)_2\cdot(C_8Br_4O_4^{2-})]$ Salt, (7) To an ethanol-distilled water solution (v/v = 1:1, 10 mL) containing 3,5-Dimethylpyrazole (19.2 mg, 0.20 mmol) was added H_2-TBTA (42.8 mg, 0.10 mmol) with constant stirring for 15 min. The clear and homogeneous solution was slowly evaporated at room temperature, and block colorless crystals were obtained two weeks later. The crystals were picked up from the mother liquor and washed with acetone-distilled water solution (v/v = 1:1), and dried under vacuum. Crystals were obtained in 58% yield by filtration and were found to be suitable for single-crystal X-ray diffraction analysis. m.p.: 260℃. Anal. Calcd (%) for $C_{18}H_{18}Br_4N_4O_4$ **(7)**: C 32.05, H 2.67, N 8.31; found : C 31.84, H 2.88, N 8.20. IR (KBr pellet, cm^{-1}) : 3458(m), 3430(m), 3139(w), 2982(m), 2917(m), 2680(m), 1723(m), 1613(s), 1464(m), 1422(s), 1362(m), 1331(s), 1306(s), 1232(s), 1160(m), 1083(s), 1016(m), 980(m), 890(m), 849(m), 816(m), 786(m), 727(m), 695(m), 578(s), 560(s), 523(m).

Synthesis of $[(C_6H_5N_2^+)_2\cdot(C_8Br_4O_4^{2-})\cdot(C_8H_2Br_4O_4)]$ Salt, (8) A solution of H_2-TBTA (42.8 mg, 0.10 mmol) was prepared in 5 mL of ethanol. 5mL distilled water solution of 4-Cyanopyridine (5.2 mg, 0.05 mmol) was added to the above solution. The resulting solution was stirred for 15 min and kept at room temperature for crystallization. Colorless, block crystals were gained after one week. The obtained crystals were separated from the mother solution by filtration, washed with ethanol-distilled water solution (v/v = 1:1), and dried under vacuum. Crystals were obtained in 58% yield by filtration and were found to be suitable for single-crystal X-ray diffraction analysis. m.p.: 276 ℃ . Anal. Calcd (%) for $C_{28}H_{12}Br_8N_4O_8$ **(8)**: C 28.68, H 1.02, N 4.78; found : C 28.54, H 1.48, N 4.56. IR (KBr pellet, cm^{-1}) : 3436(m), 3109(w), 3060(w), 2490(w), 1949(w), 1729(m), 1634(s), 1497(m), 1381(m), 1333(m), 1308(s), 1278(s), 1254(s), 1212(s), 1085(m), 1077(m), 958(m), 835(s), 774(m), 753(m), 734(m), 721(w), 657(w), 577(s), 555(m), 523(m), 467(s).

X-ray data collection and structure determinations

Crystallographic diffraction data of complexes **1-8** were recorded on an Agilent Technologies Gemini A Ultra Atlas CCD with graphite-monochromatic Mo-Kα radiation (λ=0.71073 Å) at 293 K. Absorption corrections were applied using multi-scan technique. There was no evidence of crystal decay during the data collection for all complexes. All the structures were solved by Direct Method of SHELXS-97 and refined by full-matrix least-squares techniques based on F^2 with the SHELXL-97[15] crystallographic software package. The hydrogen atoms were placed at calculated positions and refined as riding atoms with isotropic displacement parameters. The crystallographic data for **1-8** have been deposited at the Cambridge Crystallographic Data Centre with CCDC reference numbers 1016043-1016050 and are given in Table **1**.

Results and discussion

Preparation of compounds 1-8

In our initial crystallizations, we varied the stoichiometries of tetrabromoterephthalic acid and base-type reagents (1:2, 1:1, and 1:2) in parallel solution experiments. However, for these three different ratios, we obtained eight novel crystals.

Crystallization of tetrabromoterephthalic acid with 1H-Benzotriazole(1:2), 1H-Benzimidazole(1:1), 8-Hydroxyquinoline(1:2), 5-Nitro-1,10-phenanthroline(2:1), 4,6-Dihydroxypyrimidine(2:1), 2,4-Dimethylimidazole(1:1), 3,5-Dimethylpyrazole(1:2), 4-Cyanopyridine (2:1) results in crystals. These crystals structures of all eight materials (**1-8**) were carried out in different ratios and the same solvent. Eight new solids were obtained from different solvent combinations: two cocrystals: with

PAPER

Table 1 Crystal data and structure refinement summary for compounds **1-8**

Compound	1	2	3	4	5	6	7	8
Empirical formula	$C_{28}H_{14}Br_8N_6O_8$	$C_{30}H_{20}Br_8N_4O_{10}$	$C_{26}H_{22}Br_4N_2O_9$	$C_{32}H_{16}Br_4N_6O_8$	$C_{16}H_{14}Br_4N_4O_{10}$	$C_{34}H_{22}Br_{12}N_4O_{12}$	$C_{18}H_{18}Br_4N_4O_4$	$C_{28}H_{12}Br_8N_4O_8$
M	1201.65	1235.70	826.09	932.11	741.91	1637.36	673.96	1171.62
Crystal system	monoclinic	triclinic	triclinic	monoclinic	monoclinic	triclinic	triclinic	triclinic
Space group	$P2_1/c$	$P\bar{1}$	$P\bar{1}$	$P2_1/c$	$P2_1/n$	$P\bar{1}$	$P\bar{1}$	$P\bar{1}$
a/Å	11.5626(5)	8.9459(10)	10.2368(6)	17.4367(5)	7.8320(4)	9.0669(4)	8.1803(8)	8.8990(5)
b/Å	13.4148(4)	9.0271(9)	11.7277(7)	11.5949(2)	16.5732(7)	11.1569(4)	8.7685(7)	9.0236(7)
c/Å	11.3223(5)	12.5435(11)	12.9747(7)	18.1466(11)	8.9252(4)	12.8684(4)	8.9983(10)	12.0472(8)
α/°	90	72.408(9)	72.509(5)	90	90	106.546(3)	115.443(10)	105.180(7)
β/°	100.498(5)	87.358(9)	86.189(5)	121.166(3)	100.132(4)	106.524(4)	102.074(9)	109.306(6)
γ/°	90	73.572(10)	73.802(5)	90	90	100.289(4)	91.498(8)	96.573(6)
V/ Å^3	1726.81(12)	925.31(18)	1426.41(15)	3139.3(2)	1140.44(9)	1147.58(9)	565.01(11)	859.41(12)
Z	2	1	2	4	2	1	1	1
T/K	293	293	293	293	293	293	293	293
D_c/g cm^{-3}	2.311	2.218	1.923	1.972	2.161	2.369	1.981	2.264
μ/mm^{-1}	9.348	8.728	5.699	5.193	7.119	10.533	7.155	9.386
F(000)	1136.0	588.0	808.0	1816.0	716.0	770.0	326.0	552.0
h, k, lmax	13,15,13	10,10,14	14,16,18	20,13,21	10,23,12	10,13,15	9,10,10	12,12,16
R_1[a]	0.0352	0.0366	0.0400	0.0382	0.0388	0.0322	0.0308	0.0612
wR_2[a](all data)	0.0708	0.0829	0.0808	0.0931	0.0813	0.0610	0.0729	0.1661
S(GOF on F^2)	1.020	1.041	0.999	1.036	1.064	1.018	1.082	1.033

[a] $R_1=\Sigma\Delta F_o\Delta-\Delta F_c\Delta/\Sigma\Delta F_o\Delta$. [b] $wR_2=[\Sigma w(F_o^2-F_c^2)^2/\Sigma w(F_o^2)^2]^{1/2}$.

Table 2 Characteristics of hydrogen-bond geometries observed in the crystal structures of **1-8**

D-H···A (Å) (symmetry code)	D-H(Å)	H···A(Å)	D···A(Å)	D-H···A (deg)
1O1–H1A···O4 (1+x, y,–1+z)	0.989	1.636	2.618	171.3
N3–H3···O4 (2–x,1–y, –z)	0.815	2.012	2.775	155.4
N1–H1···O3 (1+x,y, –1+z)	1.021	1.594	2.614	176.3
2O4–H4···O2 (x,1+y,z)	0.820	1.752	2.566	171.3
O5–H5B···O1 (x,1+y,z)	0.850	1.949	2.785	167.2
N2–H2···O5 (x,1+y,z)	0.860	1.885	2.731	167.2
N1–H1···O2 (x,1+y,1+z)	0.860	1.864	2.696	162.3
O5–H5A···Br1 (x,1+y,z)	0.850	3.146	3.559	112.5
3O9–H9A···O2 (x, y, z)	0.850	1.964	2.812	175.1
O9–H9B···O3 (x,y,1+z)	0.850	2.026	2.872	173.2
O8–H8B···O9 (x, –1+y,z)	0.787	1.966	2.732	164.2
O8–H8A···O7 (1–x,1–y, –z)	0.747	2.011	2.754	173.2
O6–H6···O1 (x,y,z)	0.820	1.689	2.508	177.3
C37–H37···Br1 (x,y,1+z)	0.930	3.110	3.769	129.4
4O4–H4···N4 (–x, –y, –z)	0.814	1.863	2.674	174.2
C50–H50···O7 (x,y,z)	0.930	2.812	3.440	125.9
C46–H46···O3 (x,y,1+z)	0.930	2.877	3.753	157.5
5N1–H1···O3 (–x, –y, –1–z)	0.860	1.870	2.716	167.3
O3–H3A···O5 (1–x,1–y, –z)	0.850	1.944	2.754	159.0
N2–H2···O5 (1–x,1–y, –z)	0.860	1.862	2.717	172.7
O2–H2A···O4 (x,2+y,z)	0.820	1.727	2.523	163.3
6O6–H6···O2 (1+x,y,z)	0.820	1.806	2.621	172.4
O3–H3···O1 (x,2+y,z)	0.820	1.672	2.491	177.6
N1–H1···O2 (x,2+y,z)	0.860	1.981	2.827	167.8
N2–H2···O4 (1+x,y,z)	0.860	1.991	2.814	159.9
7N2–H2···O1 (1+x,y,z)	0.860	1.824	2.655	161.8
C14–H14B···O2 (1+x,y,z)	0.960	2.488	3.384	155.4
C19–H19A···O2 (1+x,y,z)	0.960	2.839	3.384	116.9
C19–H19C···O2 (1+x,y,z)	0.960	3.324	3.729	107.6
8C30–H30···O4 (x,y,1+z)	0.930	2.690	3.221	117.0
C32–H32···N2 (–x, –y, –z)	0.930	2.470	3.361	160.5
O4–H4···O1 (x,y,z)	0.820	1.755	2.537	158.7
N1–H1···O1 (1+x,y,z)	1.159	1.446	2.571	161.2

phenanthroline **(4)** and 4,6-Dihydroxypyrimidine **(5)**; two hydrous salts: with 1H-Benzimidazole **(2)**, 8-Hydroxyquinoline **(3)**; four salts: 1H-Benzotriazole **(1)**, 2,4-Dimethylimidazole **(6)**, 3,5-Dimethylpyrazole **(7)**, 4-Cyanopyridine **(8)**. However, they exhibit many common features, especially in the formation of halogen bonds. Be just like most of the supramoleculars, these crystals contain a great deal of hydrogen bond networks in which the tetrabromoterephthalic acid and base components form a series of possible synthons. The schematic representations of different kinds of hydrogen-bonding synthons I–XIII related to this work are summarized in **Scheme 2**. More synthons XIV–XXXI about this work are displayed in supporting information. The crystallographic parameters are summarized in **Table 1**. Hydrogen-bond geometries of **1-8** are listed in **Table 2**. Now we discuss the structural aspects of these new multi-component crystals.

Structural description of [(H_2-BTAH)$_2$·(TBTA)·(H_2-TBTA)] (1)

The results of X-ray crystallographic analysis revealed that complex **1** crystallizes in monoclinic *C*2/*c* space group (see Table 1). The asymmetric unit of **1** consists of one H_2-BTAH$^+$ cation, half a molecule of H_2-TBTA molecule, and half of a TBTA^{2-} dianion (Figure 1a). The tetrabromoterephthalic acid molecule is fully deprotonated with one hydroxyl proton transferred to the 1H-Benzotriazole molecule. The state of the carboxylic moiety (neutral or ionic) can be found through the C–O and C=O bond distances. The lengths of two C–O bonds for tetrabromoterephthalic acid molecule are obviously different (1.300 Å for C–OH and 1.211 Å for C=O), while the two C–O bonds for tetrabromoterephthalic acid dianion are very similar (1.254 Å and 1.252 Å) showing that one acid is neutral and the other one is fully deprotonated. The exocyclic bond lengths C20–C24 and C17–C22 are elongated to 1.506 Å and 1.518 Å, longer than those of cyclic C–C bonds (average 1.389 Å). The bond lengths C-Br are on average 1.883 Å. Within the 1H-Benzotriazole subunit, the triazole ring deviate by 1.523° from the benzene ring. Within the acid molecule and acid dianion components, the dihedral angle between two carboxyl planes is 6.966°. Within the tetrabromoterephthalic acid subunits, the

carboxyl plane and the benzene ring deviate by 80.529° and 81.103°, respectively.

Complex **1** exhibits a one-dimensional chain in the Figure 1b. These acid molecules are linked through the O1–H1A···O4 hydrogen bonds, and form oxygen-hydrogen-oxygen balanced perfectly in a V-shaped at a 110.928(2)° degree angle. Furthermore, the adjacent 1D chains are assembled into 2D layers in the *ab*-plane via N–H···O interactions between acid and base molecules, which is shown in the Figure 1c. In order to display more intuitive and clear, we show the 1D chains in pink and the 1H-Benzotriazole molecules in bright green, which is shown in the Figure 1d. Significantly, the adjacent benzene rings of the 2D layers are almost parallel (the dihedral angle between them is 3.450°), and the distance between the central point of the benzene rings is 3.6439(2) Å. It is within the range of π-π stacking interactions (3.3-3.8 Å), hence there exist π-π stacking interactions. Further analysis of the crystal packing indicated that the π-π stacking interactions link two adjoining sheets to give a 3D network structure (Figure 1e). The Figure 1f provides the detailed analysis of the π-π stacking interactions of the 3D network. Synthons I $R^4_4(16)$ and XIV $R^8_8(52)$ are formed properly and shown in Scheme 2.

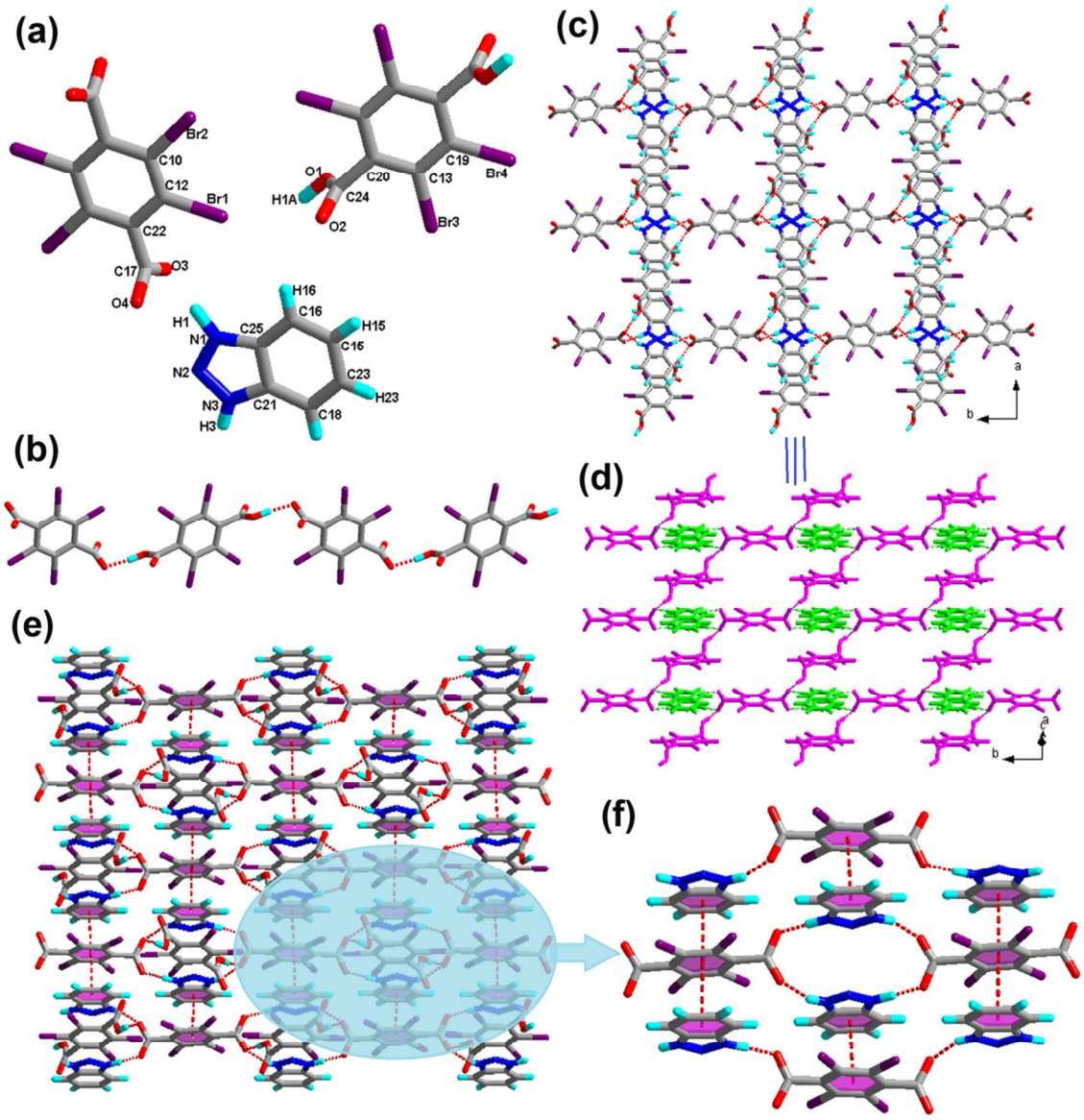

Figure 1. (a) Molecular structure of 1 with atom labeling of the asymmetric unit; (b) 1D supramolecular tape via hydrogen bonds (the hydrogen bonds are indicated as broken lines in this and the subsequent figures); (c) Perspective view of the 2D hydrogen-bonded layer; (d) The resultant 2D layer in two colours; (e) 3D network via π–π stacking interactions; (f) View of the π–π stacking interactions of H_2-TBTA molecular and 1H-BT belong to different layer. (O, red; N, blue; C, gray; H, turquoise, Br, violet in this and the subsequent figures).

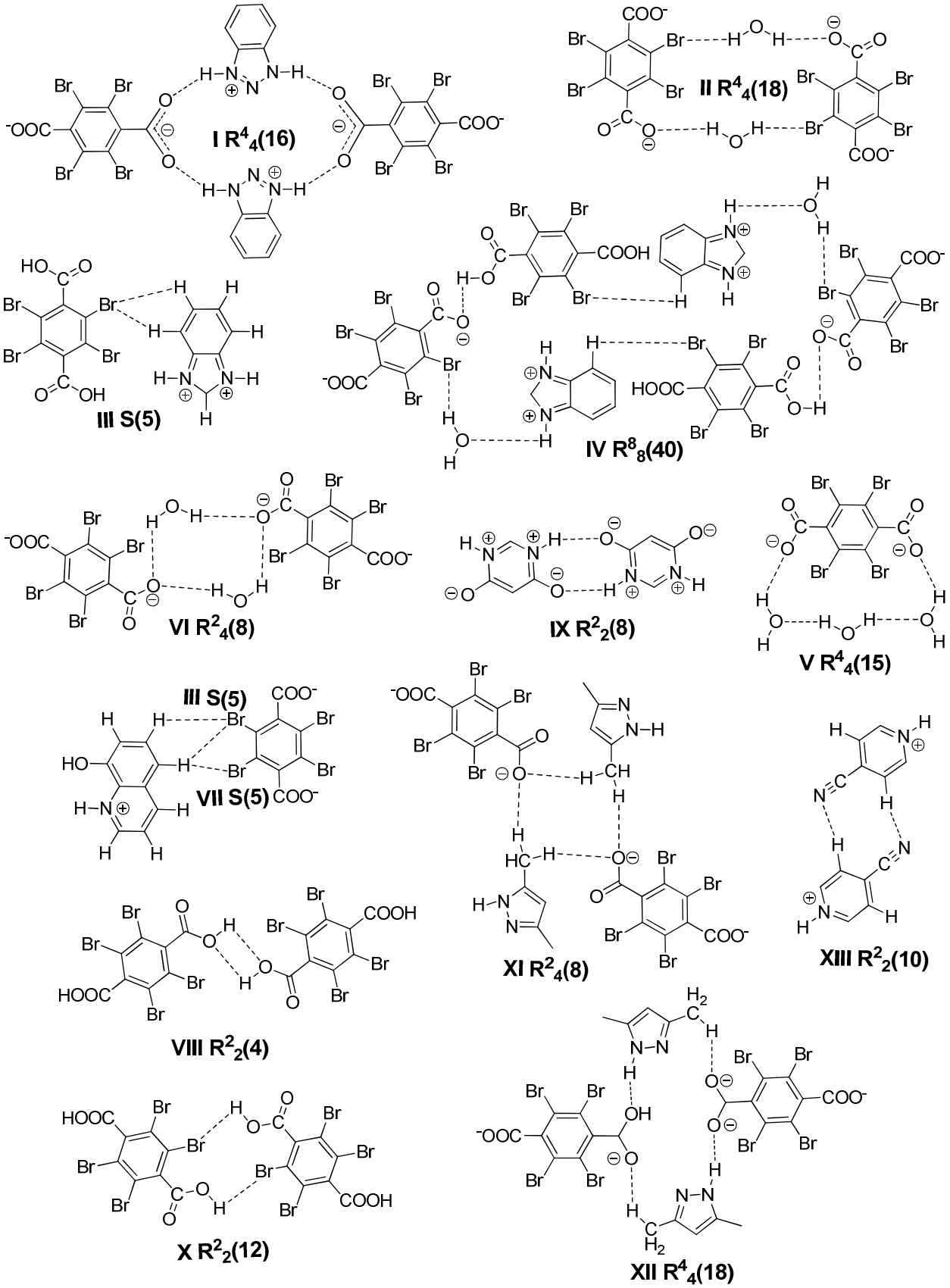

Scheme 2 Supramolecular synthons

Structural description of [(H_2-Bim)$_2$·(TBTA)·(H_2-TBTA)·2H_2O] (2) Complex **2** crystallizes in the triclinic system with *P*ī space group. The asymmetric unit of **2** contains one H_2-Bim$^+$ cation, half a molecule of H_2-TBTA molecule, half of a TBTA^{2-} dianion and one H_2O molecule (see Table 1). Within **2**, similar to compound **1**, the tetrabromoterephthalic acid molecule is fully deprotonated with one hydroxyl proton transferred to the H-Bim molecule. The state of the carboxylic moiety (neutral or ionic) can be found through the C–O and C=O bond distances. The lengths of two C–O bonds for tetrabromoterephthalic acid molecule are obviously different (1.304 Å for C–OH and 1.205 Å for C=O), while the two C–O bonds for tetrabromoterephthalic acid dianion are very similar (1.262 Å and 1.228 Å) showing that one acid is neutral and the other one is fully deprotonated. The exocyclic bond lengths C4–C19 and C8–C11 are elongated to 1.518 Å and 1.525 Å, longer than those of cyclic C–C bonds (average 1.390 Å). The bond lengths C–Br are on average 1.890 Å. Within the H-Bim subunit, the imidazole ring deviate by 0.735° from the benzene ring. Within the acid molecule and acid dianion components, the dihedral angle between two carboxyl planes is 73.335°. Within the tetrabromoterephthalic acid subunits, the carboxyl plane and the benzene ring deviate by 84.175° and 85.190°, respectively.

It was found that salt **2**, each tetrabromoterephthalic acid dianion interacts with an acid molecule forming O4–H4···O2 hydrogen bonds with –OH and –COO$^-$ groups. Thus, a one-dimensional acid chain (Figure. 2b) is formed, which is a quite usual feature of this type of recognition process that was observed in earlier examples, too. However, the interaction between adjacent chains and the resulting two-dimensional arrangement is quite fascinating. The adjacent 1D chains are interconnected by base and the water molecule via the hydrogen bonds O–H···O and N–H···O to form a two-dimensional (2D) layer (Figure 2c). The 2D sheets in **2** are linked by the hydrogen bonds N–H···O, O–H···O and weak O–H···Br interactions to form supramolecular 3D network (Figure 2d). For displaying more intuitive and clear, we presented the 2D layered structure in different colors - pink and bright green alternately, which is showed in the Figure 2e. In addition, six types of hydrogen-bonds patterns, noted as synthons II $R^4_4(18)$, III S5, XVI $R^6_6(20)$, XVII $R^8_8(40)$, and XV $R^8_{10}(52)$, are observed in this 3D array

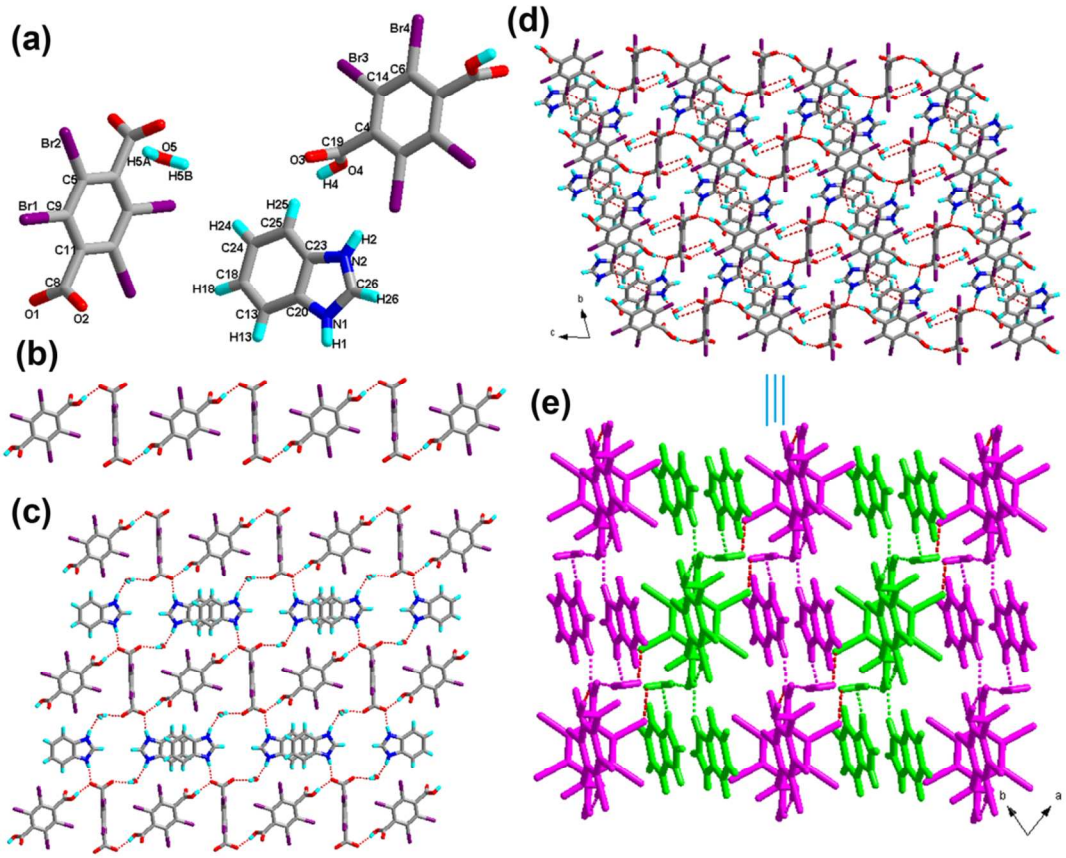

Figure 2. (a) Molecular structure of 2 with atom labeling of the asymmetric unit; (b) 1D supramolecular tape via hydrogen bonds (the hydrogen bonds are indicated as broken lines in this and the subsequent figures); (c) Perspective view of the 2D hydrogen-bonded layer; (d) The resultant 3D network; (e) The resultant 3D layer in two colours.

Structural description of [(H-8-HQ)$_2$·(TBTA)·3H_2O] (3) X-ray determination revealed that complex **3** crystallizes in triclinic *P*ī space group (see Table 1). The asymmetric unit of **3** is comprised of two H-8-HQ$^+$ cation, two half of a TBTA^{2-} dianion and three independent H_2O molecules (Figure 3a). The tetrabromoterephthalic acid molecule is fully deprotonated with one hydroxyl proton transferred to the H-8-HQ molecule. The exocyclic bond lengths C32–C35and C24–C41 are elongated to 1.526 Å and 1.527 Å, longer than the cyclic C–C bonds (average 1.387 Å). The cyclic C–N bond

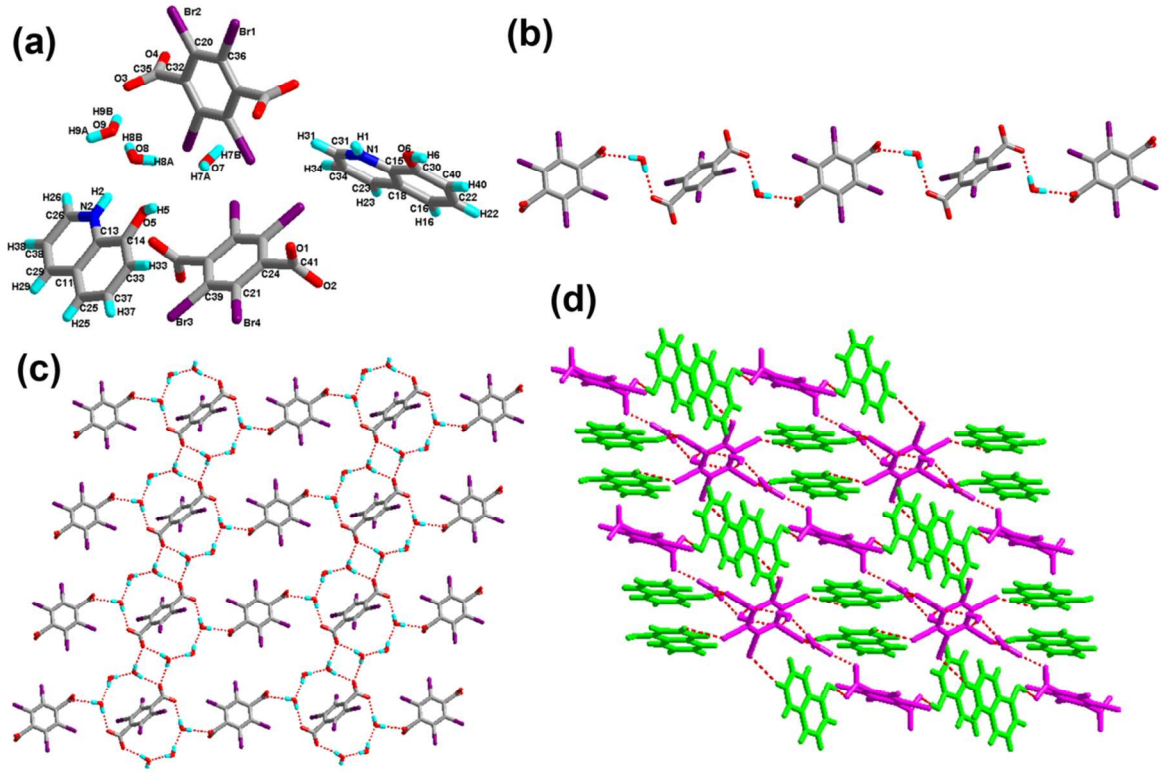

Figure 3. (a) Molecular structure of 3 with atom labeling of the asymmetric unit; (b) 1D supramolecular tape via hydrogen bonds (the hydrogen bonds are indicated as broken lines in this and the subsequent figures); (c) Perspective view of the 2D hydrogen-bonded layer; (d) The resultant 3D network; (e) The resultant 3D layer in two colours.

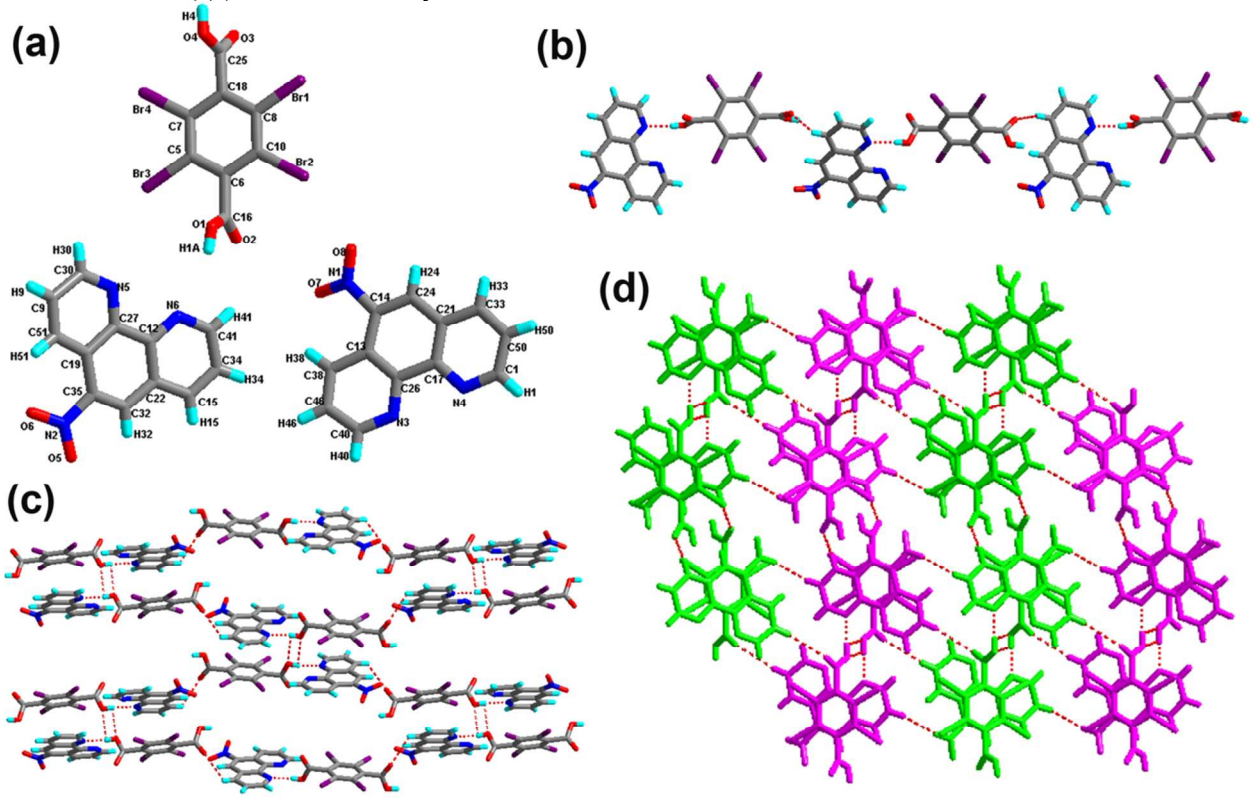

Figure 4. (a) Molecular structure of 4 with atom labeling of the asymmetric unit; (b) 1D supramolecular tape via hydrogen bonds (the hydrogen bonds are indicated as broken lines in this and the subsequent figures); (c) Perspective view of the 2D hydrogen-bonded layer; (d) The resultant 3D layer in two colours.

lengths are on average 1.342 Å, and the C–Br bond lengths are on average 1.890 Å. Within the acid anion components, the dihedral angle between the two benzene rings is 56.929°. The dihedral angles between the pyridine ring and the benzene ring of the 8-hydroxyquinoline cation molecules are 0.727° and 1.571°, respectively.

Analysis of the crystal of **3** implies that the acid subunits and water molecules locate alternately, generating a one-dimensional infinite chain through the hydrogen bond O–H···O (Figure 3b). Meanwhile, the other water molecules act as the bridge, linking the adjacent tapes. As a consequence, these 1D chains are extended to 2D sheet, and three new hydrogen-bonded patterns marked as synthons V $R^4_4(15)$, VI $R^2_4(8)$, and XVIII $R^{12}_{12}(42)$ come into being. Furthermore, as shown in Figure 3d, there exist C–H···Br hydrogen-bonding motifs, that are, synthons XIX $R^4_4(26)$ and XX $R^6_6(23)$ extend the adjacent sheets to afford a 3D supramolecular network.

Structural description of [(5-NO_2-phen)$_2$·(H_2-TBTA)] (4) A single-crystal X-ray diffraction study reveals that complex **4** crystallizes in monoclinic system with $P2_1/c$ space group. As depicted in Figure 4a, two molecules of 5-NO_2-phen were contained in the asymmetric unit, along with one molecule of H_2-TBTA. The distances for –COOH (C16–O1, 1.302 Å, C16=O2, 1.199 Å, C25–O4, 1.288 Å, C25=O3, 1.197 Å) support the existence of nonionicacid moieties indicating co-crystal formation. The exocyclic bond lengths C6–C16 and C18–C25 are elongated to 1.516 Å and 1.523 Å, longer than those of cyclic C–C bonds (average 1.388 Å). Moreover, the exocyclic bonds lengths C14–N1 and C35–N2 are elongated to1.472 Å and 1.481 Å, longer than those of cyclic C–N bonds (average 1.336 Å). The bond length C–Br is on average 1.891 Å. As illustrated in Figure 4a, the local structure of co-crystal consists of base and acid molecules. Within the 5-nitro-1,10-phenanthroline molecule moieties, the dihedral angles between the pyridine ring and the benzene ring plane of 5-NO_2-phen are 4.108°, 3.241° (the left one), 2.285°, 1.348° (the right one), respectively. In addition, within the tetrabromoterephthalic acid subunit, the carboxyl plane and the benzene ring deviate by 77.310° and 83.354°, respectively.

In the crystal structure of **4**, the acid subunits and 5-NO_2-phen molecules locate alternately, receiving a one-dimensional chain via the hydrogen bond O–H···N and the weak hydrogen bond C–H···O, as shown in Figure 4b. These 1D chains are connected to each other to form two-dimensional layer by the O–H···O hydrogen bonds (synthons XIII $R^2_2(10)$ and XXI $R^8_{10}(56)$), which the length is 2.700 Å. Furthermore, as viewed from the *ac* plane, these 2D layers are fused together to yield a 3D network through the weak hydrogen bonds C–H···O between acid and base components from adjacent sheets (Figure 4d).

Structural description of [(4,6-DHP)$_2$·(H_2-TBTA)·2H_2O] (5) Complex **5** crystallizes in the monoclinic space group $P2_1/n$. As shown in Figure 5a, the asymmetric unit contains one 4,6-DHP, half H_2-TBTA molecule and one molecule of water, among which, The distances for –COOH (C18–O2, 1.297 Å, C=O, 1.205 Å) support the existence of nonionic acid moieties indicating co-crystal formation. However, in the molecule of 4,6-dihydroxypyrimidine depicted the intramolecular proton transfer phenomenon, the hydrogen of –OH transferred to the nitrogen of the pyrimidine ring. The exocyclic bond length C13–C18 is elongated to 1.507 Å longer than those of cyclic C–C bonds (average 1.392 Å). The bond lengths C–N and C–Br average 1.356 Å and 1.883 Å, respectively. The angle between the calculated mean planes of the carboxylate group and its attached parent benzene ring of tetrabromoterephthalic acid is 85.311°. The dihedral angle between the benzene ring and the pyrimidine ring is 38.099°

These 4,6-dihydroxypyrimidine molecule moieties and water molecules form a one-dimensional infinite hydrogen bonded chain through the O–H···O and N–H···O, which is shown in Figure 5b. Furthermore, these 1D chains further join together via the interaction N2–H2···O5, meanwhile, synthons IX $R^2_2(8)$and XXII $R^8_{10}(32)$ are observed in this structure. As a consequence, 2D sheet network is formed through these synthons, as depicted in Figure 5c. In addition, these 2D sheets are extended to a 3D framework (Figure 5d) as viewed from the *bc* plane, through the O–H···O bond between acid and base components from adjacent sheets. For displaying more intuitive and clear, we presented the 2D layered structure in bright green and the tetrabromoterephthalic acid moieties in pink, which is showed in the Figure 5e.

Structural description of [(H_2-2,4-DMI)$_2$·(TBTA)·(H_2-TBTA)$_2$] (6) Complex **6** crystallizes in triclinic space group $P\bar{1}$ (see Table 1). As depicted in Figure 6a, the asymmetric unit of **6** contains one H-2,4-DMI^+ cation, two half H_2-TBTA, and half $TBTA^{2-}$ anion. In **6**, one of tetrabromoterephthalic acid was deprotonated to from a dianion compound. Meanwhile, 2,4-dimethylimidazole was protonate to obtain the monocation compound. In the absence of hydrogen bonding and other electronic perturbations, the C–O bond lengths should be equal because of resonance. The formation of single or multiple hydrogen bonds at one oxygen atom should cause the associated C–O bond to lengthen. It is clear that the average distances for C–O (1.248 Å) in the tetrabromoterephthalic acid anion is less than the single bond C–O (1.307 Å) and greater than the double bond C=O (1.205 Å) in the carboxylic acid group of the tetrabromoterephthalic acid molecule. This supports our assignment of the tetrabromoterephthalic acid dianions. The C–N bond lengths are average 1.348 Å. The exocyclic C–C bond lengths (average 1.513 Å) are longer than cyclic C–C bond lengths (average 1.388 Å). The exocyclic C–Br bond lengths are on average 1.884 Å. The angle between the tetrabromoterephthalic acid molecules and tetrabromoterephthalic acid anion are 82.948° and 13.103°, respectively.

These tetrabromoterephthalic acid dianion and molecule moieties form a linear infinite hydrogen bonded chain with adjacent –COOH and $–COO^-$ groups of neighboring moieties with the anion and molecule moieties arranged alternately, running parallel to the *a*-axis as shown in Figure 6b. Furthermore, the adjacent 1D chains connected via the hydrogen bond O–H···O. On the basis of these connection modes, these 1D chains are linked to generate a 2D layer structure (Figure 6c). To further understand the structure of **6**, the 3D network was carried out. As depicted in Figure 6d, the 2D sheets were displayed in pink and the H-2,4-DMI molecules were showed in bright green. They connected through the N–H···O to generate 3D supramolecular structure. In addition, four types of synthons, notated as X $R^2_2(12)$, XXIII $R^6_4(32)$, XXIV $R^6_6(29)$and XXV $R^6_6(39)$ are observed in this 3D array.

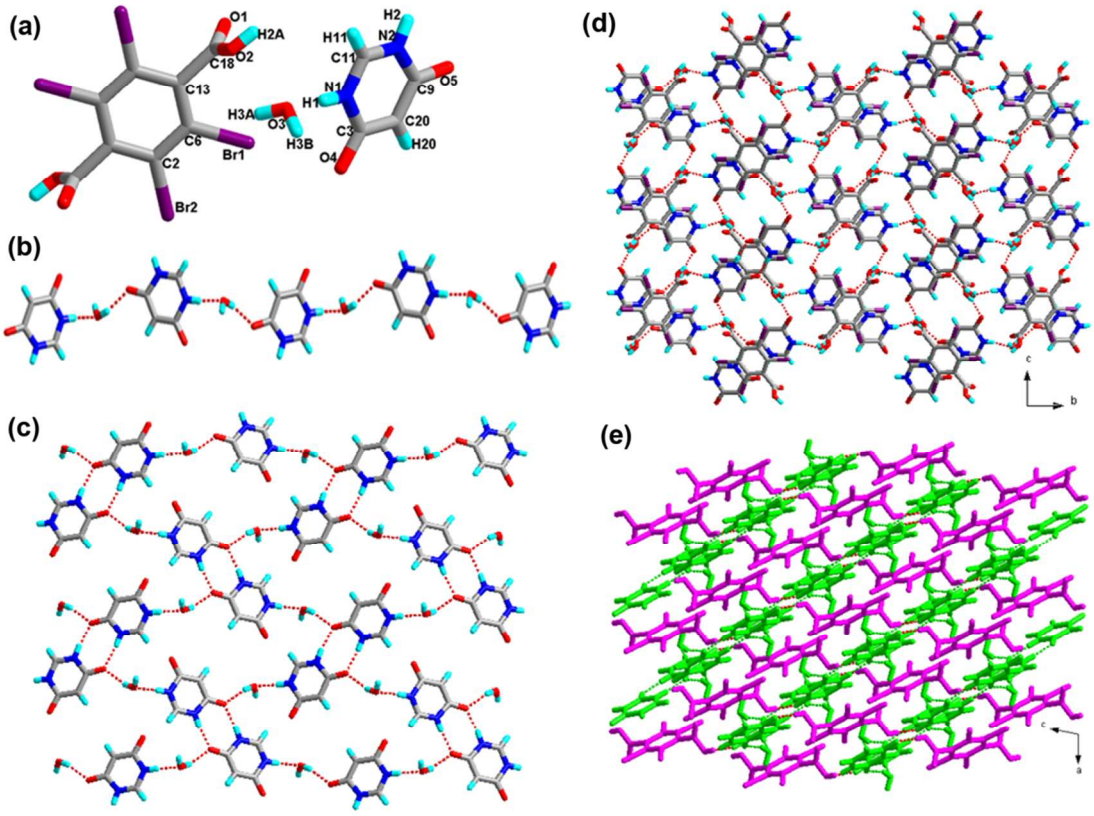

Figure 5. (a) Molecular structure of 5 with atom labeling of the asymmetric unit; (b) 1D supramolecular tape via hydrogen bonds (the hydrogen bonds are indicated as broken lines in this and the subsequent figures); (c) Perspective view of the 2D hydrogen-bonded layer; (d) The resultant 3D network; (e) The resultant 3D layer in two colours.

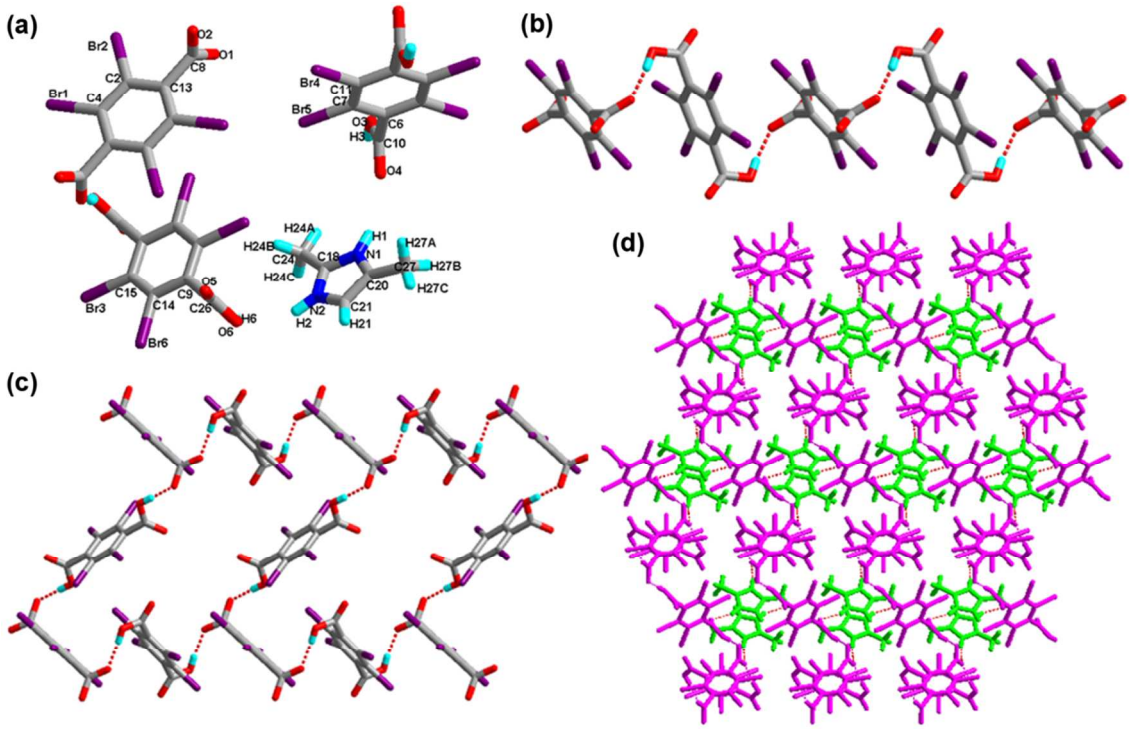

Figure 6. (a) Molecular structure of 6 with atom labeling of the asymmetric unit; (b) 1D supramolecular tape via hydrogen bonds (the hydrogen bonds are indicated as broken lines in this and the subsequent figures); (c) Perspective view of the 2D hydrogen-bonded layer; (d) The resultant 3D network; (e) The resultant 3D layer in two colours.

Structural description of [(H_2-3,5-DMP)$_2$·(TBTA)] (7) X-ray single crystal diffraction revealed that compound **7** crystallizes in the triclinic space group *P*$\bar{1}$ (see Table 1). The asymmetric unit of the structure for compound **7** is composed of one H-3,5-DMP^+ cation and half $TBTA^{2-}$ anion. As shown in Figure 7a, 3,5-dimethylpyrazole accepts one hydrogen from half a tetrabromoterephthalic acid molecule. The acidic –COOH hydrogen on tetrabromoterephthalic acid has been transferred to the basic –N– moiety of 3,5-dimethylpyrazole. In the absence of hydrogen bonding and other electronic perturbations, the C–O bond lengths should be almost equal in the molecular of tetrabromoterephthalic acid (O1–C4, 1.243 Å; O2–C4, 1.244 Å) because of resonance. The exocyclic C–C bond lengths (C4–C8, 1.534 Å) are longer than cyclic C–C bond lengths (average 1.389 Å). The exocyclic C–Br bond lengths are on average 1.891 Å. The bond lengths C–N average 1.338 Å. The dihedral angle between the benzene ring of tetrabromoterephthalic acid anion and the pyrazole ring of the 3,5-dimethylpyrazole anion is 37.206°.

Analysis of the crystal of **7** implies that the acid subunits and base molecules locate alternately, generating a one-dimensional infinite chain through the hydrogen bond N–H···O and the weak interaction C–H···O (Figure 7b). Furthermore, the adjacent 1D chains connected to each other through the C–H···O. As a consequence, these 1D chains are extended to a 2D sheet (shown in Figure 7c), and three new hydrogen-bonded patterns marked as XXVI $R^6_5(25)$ comes into being, Significantly, as shown in Figure 7d, there exist the weak hydrogen bonds C–H···O, that are, these 2D layers extend the adjacent sheets to afford a 3D supramolecular network. Synthons XI $R^2_4(8)$, XII $R^4_4(18)$, XXVII $R^4_4(28)$ and XXVIII $R^4_4(30)$ are formed properly and shown in **Scheme 2** and supporting information.

Structural description of [(H-4-CNpy)$_2$·(TBTA)·(H_2-TBTA)] (8) Complex **8** crystallizes in the triclinic crystal system with *P*$\bar{1}$ space group, and the asymmetric unit is found to be composed of one H-4-$CNpy^+$ cation, half H_2-TBTA and half $TBTA^{2-}$ anion. As shown in Figure 8a, the state of the carboxylic moiety (neutral or ionic) can be found through the C–O and C=O bond distances. The lengths of two C–O bonds for tetrabromoterephthalic acid molecule are obviously different, which is 1.304 Å for C–OH and 1.195 Å for C=O. While the two C–O bonds for tetrabromoterephthalic acid anion are very similar (1.207 Å and 1.303 Å) showing that one acid is neutral and the other is fully deprotonated. The tetrabromoterephthalic acid molecule is fully deprotonated with one hydroxyl proton transferred to the 4-cyanopyridine. The exocyclic bond lengths C3–C8, C12–C24 and C13–C27 are elongated to 1.510 Å, 1.527 Å and 1.439 Å, respectively, which is longer than those of the cyclic C–C binds (average 1.380 Å). The cyclic bond lengths C–N are average 1.327 Å, and the exocyclic bond lengths C–Br are average 1.883 Å. The dihedral angle between the two benzene rings of the acid subunits is 75.865°. In addition, the dihedral angles between the pyridine ring and the two benzene rings are 0.828° and 75.282°, respectively.

To further understand the structure of **8**, the one-dimensional chain was carried out. In **8**, the adjacent 4-cyanopyridine molecules were connected to form a new hydrogen-bonded ring with the graph-set of XIII $R^2_2(10)$. Meanwhile, the synthons XIII $R^2_2(10)$ and H_2-TBTA molecules locate alternately, generating a 1D infinite chain via the hydrogen bond C–H···O (Figure 8b). tetrabromoterephthalic acid anions act as bridge linking the adjacent 1D chains through O–H···O. As a consequence, these 1D chains are extended to a 2D sheet, and new hydrogen-bonded pattern marked as synthons XXIX $R^6_6(30)$, XXX $R^4_6(30)$, XXXI $R^6_8(26)$ come into being. Such neighboring 2D layers are further cross-linked via the N1–H1···O1 hydrogen bond, generating a 3D structure along *a*-axis. In the Figure 8d, the 2D layers were depicted in different colors, so the connection between each other displayed more clearly.

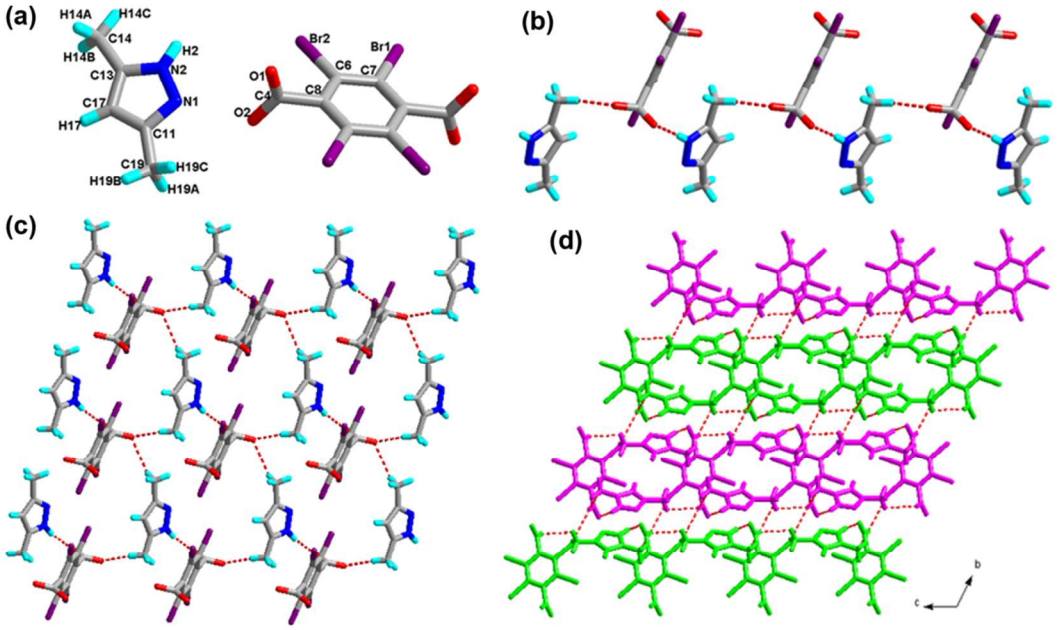

Figure 7. (a) Molecular structure of 7 with atom labeling of the asymmetric unit; (b) 1D supramolecular tape via hydrogen bonds (the hydrogen bonds are indicated as broken lines in this and the subsequent figures); (c) Perspective view of the 2D hydrogen-bonded layer; (d) The resultant 3D network; (e) The resultant 3D layer in two colours.

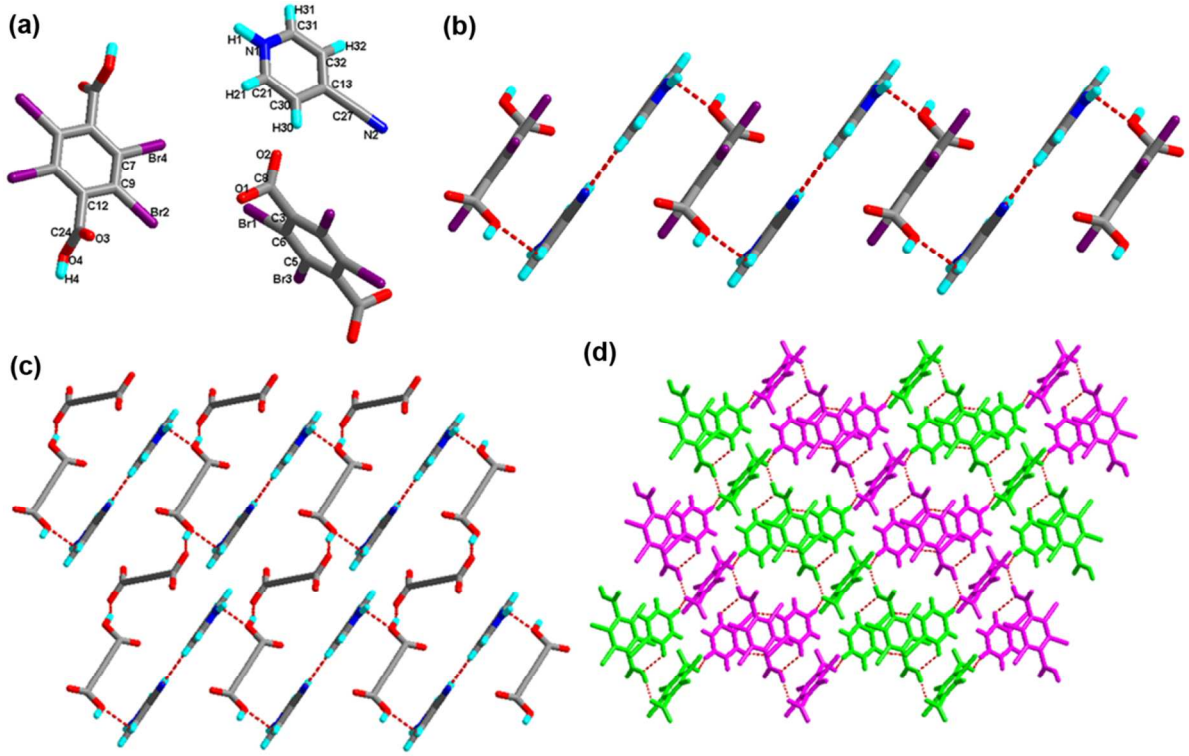

Figure 8. (a) Molecular structure of 8 with atom labeling of the asymmetric unit; (b) 1D supramolecular tape via hydrogen bonds (the hydrogen bonds are indicated as broken lines in this and the subsequent figures); (c) Perspective view of the 2D hydrogen-bonded layer; (d) The resultant 3D network; (e) The resultant 3D layer in two colours..

Thermal stability analysis

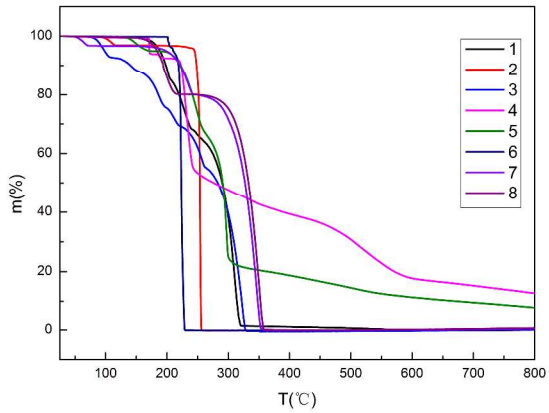

Figure 9. The TGA curves of complexes **1-8**

All complexes **1-8** are stable in air and can maintain their structural integrity at ambient conditions for a long time. In order to examine the thermal stability of all complexes, the TGA and DSC were carried out between room temperature and 900℃ in nitrogen atmosphere. The DSC traces and TGA data for the crystals are presented in Supporting Information. TGA experiments were implemented to investigate their thermal stability. The behaviors of the eight complexes are depicted in Figure 9. As for complex **6**, the TGA results indicate that they remain intact until 218℃, and then there are a sharp weight loss ending at 260℃.(peaks: 225.1℃ for crystal **6**). The weight loss of complex **6** up to 99.96% to 260℃. The TGA curves of **2**, **7** and **8** indicate that there are two consecutive weight losses of the three samples. Complex **2** decomposes from 100℃ to 258℃ (peaking at 256℃), while **7** and **8** are more stable than the compound **1** and when it comes to 140 ℃ and 160 ℃, respectively, the decomposition of the framework begins. (peaking at 237℃, 351℃ and 198℃, 355℃, respectively). As for **2**, the first weight loss of 3.25% from 100 to 110 ℃ (calculated: 2.91%) corresponds to the loss of two water molecule per formula. The second weight loss of 96.87% (calculated: 97.09%) can be detected from 220 to 258℃, which is owed to decomposition of acid and base molecule. Compared with complex **1**, the TGA measurement of **7** shows a weight loss of 30.51% in the temperature range 110℃ to 155℃, which corresponds to the loss of 3,5-dimethylpyrazole molecule, and the second weight loss represented the loss of acid components (calculated: 71.47%, found: 80.09%). The TGA measurement of **8** indicates that the complex does not melt and is stable up to 145℃, at which temperature the crystal begins to decompose. The ligand 4-cyanopyridine and tetrabromoterephthlic acid molecule decompose at 145-368℃ with two peaks at 198℃ and 355℃. As for **5**, the first weight loss of 5.13% (calculated: 4.85%) from 95 to 170℃ corresponds to the loss of two water molecule per formula, the second weight loss of 27.64% from 195 to 270℃, and the third weight loss of 61.30% from 270 to 338℃. As for **1**, the first weight loss of 14.66% from 155 to

210℃, the second weight loss of 19.41% from 210 to 245℃, and the third weight loss of 65.53% from 245 to 326℃. For complex **4**, two consecutive weight losses of all substance in the 167℃-610℃ (peaking at 235℃ and 519℃, respectively). The TGA curve of complex **3** indicates that it has three trends of decomposition. The sample is stable up to 78℃ at which temperature it starts to melt and decompose. The first mass loss illustrated the loss of 7.22% (calculated: 6.54%) corresponds to the loss of three water molecule per formula, and the second mass loss represented the base molecules, and the third mass loss of 55.69% which is correspond to the acid molecules (calculated: 58.23%). Moreover, the theoretical value and practical value differ within a reasonable range. Broadly speaking, the eight frameworks have a remarkably thermal stability.

Conclusions

The self-assembled of designed molecules containing certain kinds of synthons has stimulated new efforts in the material science. Such crystal manipulations, often known through crystal engineering, are performed to yield new structural molecular solids. The successful preparation of the eight organic acid-base adducts in this paper provides novel 3D network structures by using suitable flexible ligands. These structures contribute to the extensive research into the occurrence of tetrabromoterephthalic acid compound motifs in organic solids.

From this study it can be seen that tetrabromoterephthalic acid will form organic solids with the basic molecules. With the exception of compounds **4** and **5**, for the other six complexes are formed salts by the proton transfer process. Under normal conditions, the proton of the carboxylic acid transfer to the nitrogen atoms in the basic compounds. Crystals **4** and **5** formed cocrystals and kept the original molecular structure. The strong intermolecular N–H···O and O–H···O hydrogen bonds generally exist in these structures. These interactions are responsible for the high-yielding supramolecular assembly of tetrabromoterephthalic acid and N-heterocycles into organic solids, with desire connectivities. In addition, the weak interactions C–H···O, C–H···Br and N–H···Br were observed based upon their geometric perferences and showed an equally important to the strong hydrogen bonds in these structures. There are also π-π stacking interactions in the compound **1** in which the closest separations between centers of aromatic rings is 3.644 Å. More importantly, the bromine atom played a vital important role in constructing these crystal structures, through the C–H···Br and N–H···Br hydrogen bond interactions.

It is noted that although these N-heterocycles, such as H-BTAH, 4-CNpy, H-Bim, and 4,6-DHP ligands present a planar space configuration; 8-HQ, 3,5-DMP, 2,4-DMI display a three-dimensional space configuration due to the –OH, $–CH_3$ groups, all crystal structures containing these ligands are 3D supramolecular networks. These result mainly due to the existence of the large number of hydrogen bonds (O–H···O, O–H···N, N–H···O, N–H···N, C–H···O, C–H···N, C–H···Br, N–H···Br) and Br···Br interactions present in these structures. In future studies, we will continue to research the halogens compounds and to discover the C–H···halogen and halogen···halogen interactions in the crystal construction.

Acknowledgements

This work was financially supported by the National Natural Science Foundation of China (No. 51372125, 21371105, and 21203106), and the Scientific and Technical Development Project of Qingdao (No. 13-1-4-184-jch).

Notes and references

1 (a) K. Biradha, A. Nangia, G. R. Desiraju, C. J. Carrell, and H. L. Carrell, *J. Mater. Chem.*, 1997, **7**, 1111–11221; (b) V. R. Thalladi, S. Brasselet, D. Bläser, R. Boese, J. Zyss, A. Nangia, and G. R. Desiraju, *Chem. Commun*., 1997, **19**, 1841–1842; (c) S. S. Kuduva, D. C. Craig, A. Nangia, and G. R. Desiraju, *J. Am. Chem. Soc.*, 1999, **121**, 1936–1944; (d) G. A. Hembury, V. V. Borovkov, and Y. Inoue, *Chem. Rev.*, 2008, **108**, 1–73; (e) H. Cho, L. Widanapathirana, and Y. Zhao, *J. Am. Chem. Soc*. 2011, **133**, 141–147; (f) Q. P. Duan, Y. Cao, Y. Li, X. Y. Hu, T. X. Xiao, C. Lin, Y. Pan, and L. Y. Wang, *J. Am. Chem. Soc*., 2013, **135**, 10542−10549; (g) X. F. Ji, J. Y. Li, X. Z. Yan, and F. H. Huang, *J. Am. Chem. Soc*., 2013, **135**, 74−77; (h) F. Awwadi, S. F. Haddad, R. D. Willett, and B. Twamley, *Cryst. Growth Des*., 2010, **10**, 158–164; (i) H. P. Zhou, J. H. Yin, L. X. Zheng, P. Wang, F. Y. Hao, W. Q. Geng, X. P. Gan, G. Y. Xu, J. Y. Wu, Y. P. Tian, X. T. Tao, M. H. Jiang, and Y. H. Kan, *Cryst. Growth Des*., 2009, **9**, 3789–3798; (j) G. R. Desiraju, Journal of Molecular Structure, 2003, **656**, 5–15; (k) F. T. Martins, N. Paparidis, A. C. Doriguetto, and J. Ellena, *Cryst. Growth Des*., 2009, **9**, 5283–5292.

2 (a) S. S. Kuduva, D. C. Craig, A. Nangia, and G. R. Desiraju, *J. Am. Chem. Soc*., 1999, **121**, 1936–1944; (b) F. Awwadi, S. F. Haddad, R. D. Willett, and B. Twamley, *Cryst. Growth Des*., 2010, **10**, 158–164.

3 (a) G. A. Hembury, V. V. Borovkov, and Y. Inoue, *Chem. Rev.*, 2008, **108**, 1–73; (b) X. F. Ji, J. Y. Li, X. Z. Yan, and F. H. Huang, *J. Am. Chem. Soc*., 2013, **135**, 74−77. (c) C. Y. Wang, J. G. Wang, P. Z. Li, J. K. Gao, S. Y. Tan, W. W. Xiong, B. L. Hu, P. S. Lee, Y. L. Zhao, and Q. C. Zhang. *Chem. Asian J.*, 2014, **9**, 779–783; (d) G. Li, Y. C. Wu, J. K. Gao, C. Y. Wang, J. B. Li, H. C. Zhang, Y. Zhao, Y. L. Zhao, and Q. C. Zhang. *J. Am. Chem. Soc.*, 2012, **134**, 20298−20301; (e) J. F. Zhao, G. Li, C. Y. Wang, W. Q. Chen, S. C. J. Loo, and Q. C. Zhang. *RSC Adv.*, 2013, **3**, 9653–9657; (f) G. Li, Y. C. Wu, J. K. Gao, J. B. Li, Y. Zhao, and Q. C. Zhang. *Chem. Asian J.*, 2013, **8**, 1574–1578.

4 (a) Q. P. Duan, Y. Cao, Y. Li, X. Y. Hu, T. X. Xiao, C. Lin, Y. Pan, and L. Y. Wang, *J. Am. Chem. Soc*., 2013, **135**, 10542−10549; (b) R. Chakrabarty, P. S. Mukherjee, and P. J. Stang, *Chem. Rev*., 2011, **111**, 6810–6918.

5 (a) A. S. Singh, B. Y. Chen, Y. S. Wen, C. Tsai, and S. S. Sun, *Org. Lett*., 2009, **11**, 1867−1870. (b) L. Wang, L. Zhao, L. Y. Xu, R. X. Chen, and Y. Yang, *CrystEngComm*, 2012, **14**, 6998–7008; (c) L. Wang, R. F. Xue, L. Y. Xu, X. Lu, R. X. Chen, and X. T. Tao. *Sci. China Chem*. 2012, **55**, 1228–1235. (d) B. Yang, J. C. Xiao, J. I. Wong, J. Guo, Y. C. Wu, L. J. Ong, L. L. Lao, F. Boey, H. Zhang, H.

Y. Yang, and Q. C. Zhang. *J. Phys. Chem. C*, 2011, **115**, 7924–7927; (e) Z. Q. Lin, P. J. Sun, Y. Y. Tay, J. Liang, Y. Liu, N. E. Shi, L. H. Xie, M. D. Yi, Y. Qian, Q. L. Fan, H. Zhang, H. H. Hng, J. Ma, Q. C. Zhang, and W. Huang. *ACS Nano*, 2012, **6**, 5309–5319; (f) J. C. Xiao, B. Yang, J. I. Wong, Y. Liu, F. X. Wei, K. J. Tan, X. Teng, Y. C. Wu, L. Huang, C. Kloc, F. Boey, J. Ma, H. Zhang, H. Y. Yang, and Q. C. Zhang. *Org. Lett.*, 2011, **13**, 3004–3007; (g) J. C. Xiao, Z. Y. Yin, Y. C. Wu, J. Guo, Y. H. Cheng, H. Li, Y. Z. Huang, Q. Zhang, J. Ma, F. Boey, H. Zhang, and Q. C.Zhang. *small*, 2011, **7**, 1242–1246; (h) Y. Liu, F. Boey, L. L. Lao, H. Zhang, X. G. Liu, and Q. C. Zhang. *Chem. Asian J*., 2011, **6**, 1004–1006.

6 (a) M. Yamada, R. Kanazawa, and F. Hamada, *CrystEngComm*, 2014, **16**, 2605–2614; (b) I. Saraogi, V. G. Vijay, S. Das, K. Sekar, and T. N. Guru Row, *Crystal Engineering*, 2003, **6**, 69-77; (c) C. B. Aakeröy, and A. M. Bratty, *Aust. J. Chem*., 2001, **54**, 409–421; (d) R. Chakrabarty, P. S. Mukherjee, and P. J. Stang, *Chem. Rev*., 2011, **111**, 6810–6918; (e) M. Morgan Conn, and Julius Rebek, Jr., *Chem. Rev*., 1997, **97**, 1647−1668; (f) S. Yagai, T. Nakajima, K. Kishikawa, S. Kohmoto, T. Karatsu, and A. Kitamura, *J. Am. Chem. Soc*., 2005, **127**, 11134−11139; (g) H. B. Yang, K. Ghosh, B. H. Northrop, Y. R. Zheng, M. M. Lyndon, D. C. Muddiman, and P. J. Stang, *J. Am. Chem. Soc*., 2007, **129**, 14187−14189; (h) F. F. Awwadi, R. D. Willett, and B. Twamley, *Cryst. Growth Des*., 2007, **7**, 624–632.

7 (a) N. Stanley, V. Sethuraman, P. Thomas Muthiah, P. Luger, and M. Weber, *Cryst. Growth Des*., 2002, **2**, 631–635; (b) S. Baskar Raj, P. Thomas Muthiah, G. Bocelli, R. Ollá and A. Cantoni, *Cryst. Growth Des*., 2003, **3**, 567–571; (c) R. Thaimattam, D. S. Reddy, F. Xue, T. C. W. Mak, A. Nangia, and G. R. Desiraju, *J. Chem. Soc., Perkin Trans*,. 1998, 2, 1783–1789.(d) L. Wang, L. Zhao, W. Liu, R. X. Chen, Y. X. Gu, and Y. Yang, *Sci. China Chem*., 2012, **55**, 2381–2387; (e) L. Wang, L. Zhao, R. F. Xue, X. Lu, Y.H. Wen, and Y. Yang, *Sci. China Chem.*, 2012, **55**, 2515–2522.

8 (a) J. N. Moorthy, R. Natarajan, P. Mal, and P. Venugopalan, *J. Am. Chem. Soc*., 2002, **124**, 6530−6531. (b) L. Wang, L. Zhao, M. Liu, F. Q. Liu, Q. Xiao, and Z. Hu, *Sci. China Chem*., 2012, **55**, 2523–2531; (c) L. Wang, L. Zhao, M. Liu, R. X. Chen, Y. Yang, and Y. X. Gu, *Sci. China Chem*., 2012, **55**, 2115–2122.

9 (a) B. Moulton, and M. J. Zaworotko, *Chem. Rev*., 2001, **101**, 1629−1658; (b) S. Berski, Z. Ciunik, K. Drabent, Z. Latajka, and J. Panek, *J. Phys. Chem. B*, 2004, **108**, 12327–12332; (c) M. L. Tong, Z. J. Lin, W. Lin, S. L. Zheng, and X. M. Chen, *Cryst. Growth Des*., 2002, **2**, 443–448; (d) K. Dziubek, M. Podsiadlo, and A. Katrusiak, *J. Phys. Chem. B*, 2009, **113**, 13195–13201; (e) M. Yamada, R. Kanazawa, and F. Hamada, *CrystEngComm*, 2014, **16**, 2605–2614; (f) F. F. Awwadi, R. D. Willett, and B. Twamley, *Cryst. Growth Des*., 2007, **7**, 624–632. (g) D. Cao, M. Hong, A.K. Blackburn, Z. C. Liu, J. M. Holcroft and J. F. Stoddart. *Chem. Sci.*, 2014, DOI: 10.1039/c4sc00999a.

10 F. Guthrie, *J. Chem. Soc*., 1863, **16**, 239–244.

11 (a) R. Glaser, N. J. Chen, H. Wu, N. Knotts, and M. Kaupp, *J. Am. Chem. Soc*., 2004, **126**, 4412−4419; (b) L. Wang, L. Y. Xu, R. Xue, X. Lu, R. X. Chen, X. Tao, *Sci. China Chem*., 2012, **55**, 138–144; (c) P. T. Pham, and M. M. Bader, *Cryst. Growth Des*., 2014, **14**, 916–922.

12 (a) M. Fourmigué and P. Batail, *Chem. Rev*., 2004, **104**, 5379−5418; (b) N. S. Goroff, S. M. Curtis, J. A. Webb, F. W. Foeler, and J. W. Lauher, *Org. Lett.*, 2005, **7**, 1891−1893 (c) Md. B. Zaman, K. A. Udachin, and J. A. Ripmeester, *Cryst. Growth Des*., 2004, **4**, 585–589; (d) F. Zordan, and L. Brammer, *Cryst. Growth Des*., 2006, **6**, 1374–1379; (e) R. D. Willett, F. Awwadi, and R. Butcher, *Cryst. Growth Des*., 2003, **3**, 301–311; (f) K. A. Kounavi, M. J. Manos, E. E. Moushi, A. A. Kitos, C. Papatriantafyllopoulou, A. J. Tasiopoulos, and V. Nastopoulos, *Cryst. Growth Des*., 2012, **12**, 429–444.

13 (a) F. Zapata, A. Caballero, N. G. White, T. D. W. Claridge, P. J. Costa, V. Félix, and P. D. Beer, *J. Am. Chem. Soc*., 2012, **134**, 11533−11541; (b) H. Y. Gao, X. R. Zhao, H. Wang, X. Pang, and W. J. Jin, *Cryst. Growth Des*., 2012, **12**, 4377–4387; (c) J. Viger-Gravel, S. Leclerc, I. Korobkov, and D. L. Bryce, *CrystEngComm*, 2013, **15**, 3168–3177; (d) T. J. Mooibroek and P. Gamez, *CrystEngComm*, 2013, **15**, 4565–4570; (e) X. Y. Yang, F. Wang, Q. X. Chen, L. Y. Wang, and Z. Q. Wang, *Chinese Sci. Bulletin*, 2007, **52**, 1856–1859; (f) P. Metrangolo, H. Neukirch, T. Pilati, and G. Resnati, *Acc. Chem. Res*., 2005, **38**, 386–395 .

14 (a) C. P. Li, J. Chen, and M. Du, *CrystEngComm*, 2010, **12**, 4392–4402; (b) C. P. Li, Y. L. Tian, and Y. M. Guo, *Inor. Chem. Comm.*, 2008, **11**, 1405–1408; (c) P. G. Waddell, J. O. S. Hulse, and J. M. Cole, *Acta Cryst*., 2011, **C67**, o255–o258; (d) Z. Hulvey, E. Ayala, and A. K. Cheetham, *Z. Anorg. Allg. Chem*., 2009, **635**, 1753–1757; (e) Z. Hulvey, J. D. Furman, S. A. Turner, M. Tang, and A. K. Cheetham, *Cryst. Growth Des*., 2010, **10**, 2041–2043; (f) Y. Ma, X. P. Chen, D. Cao, S. P. Yan, and D. Z. Liao, *Sci China Ser B-Chem*.,2009, **52**, 1438–1443; (g) C. Seidel, R. Ahlers, and U. Ruschewitz, *Cryst. Growth Des*., 2011, **11**, 5053–5063; (h) Z. Hulvey, E. Ayala, J. D. Furman, P. M. Forster, and A. K. Cheetham, *Cryst. Growth Des*., 2009, **9**, 4759–4765; (i) A. Orthaber, C. Seidel, F. Belaj, J. H. Albering, R. Pietschnig, and U. Ruschewitz, *Inorg. Chem*., 2010, **49**, 9350–9357; (j) R. Kitaura, F. Iwahori, R. Matsuda, S. Kitagawa, Y. Kubota, M. Takata, and T. C. Kobayashi, *Inorg. Chem*., 2004, **43**, 6522–6524; (k) L. Wang, L. Zhao, Y. J. Hu, W. Q. Wang, R. X. Chen, and Y. Yang, *CrystEngComm*, 2013, **15**, 2835–2852; (l) L. Wang, Y. J. Hu, W. Q. Wang, F. Q. Liu, and K. K. Huang, *CrystEngComm*, 2014, 16, 4142–4161.

15 (a) G. M. Sheldrick, *SHELXS-97*, *Program for the Solution of Crystal Structures*, University of Göttingen, Göttingen, Germany, 1997; (b) G. M. Sheldrick, *SHELXL-97*, *Programs for X-ray Crystal Structure Refinement*, University of Göttingen, Göttingen, Germany, 1997.